

Article

Homogeneous Crystallization of Micro-Dispensed TIPS-Pentacene Using a Two-Solvent System to Enable Printed Inverters on Foil Substrates

Indranil Bose ^{1,*}, Kornelius Tetzner ², Kathrin Borner ¹ and Karlheinz Bock ²

¹ Fraunhofer EMFT, HansasträÙe 27d, Munich 80686, Germany;

E-Mail: Kathrin.Borner@emft.fraunhofer.de

² Electronic Packaging Laboratory, Technische Universität Dresden, Dresden 01062, Germany;

E-Mails: kornelius.tetzner@tu-dresden.de (K.T.); karlheinz.bock@tu-dresden.de (K.B.)

* Author to whom correspondence should be addressed; E-Mail: Indranil.Bose@emft.fraunhofer.de;

Tel.: +49-89-5475-9190; Fax: +49-89-5475-9550.

Academic Editor: Mostafa Bassiouni

Received: 30 June 2015 / Accepted: 10 August 2015 / Published: 21 August 2015

Abstract: We report on a micro-dispensing system for 6,13-Bis(triisopropylsilylethynyl) pentacene (TIPS-pentacene) to enable homogenous crystallization and uniform film morphology of the dispensed droplets using a two-solvent mixture along with the use of an insulating binder. This solution composition results in a controlled evaporation of the droplet in ambient air such that the Marangoni flow counteracts the outward convective flow to enable uniform radial crystal growth from the edge towards the center of the drops. The consequence of this process is the high degree of uniformity in the crystallization of the drops, which results in a reduction in the performance spread of the organic field effect transistors (OFET) created using this process. The addition of the insulating binder further improves the reduction in the spread of the results as a trade-off to the reduction in mobility of the transistors. The transfer curves of the OFETs show a tight grouping due to the controlled self-alignment of the TIPS-pentacene crystals; this repeatability was further highlighted by fabricating *p*-type inverters with driver to load ratios of 8:1, wherein the output inverter curves were also grouped tightly while exhibiting a gain of greater than 4 in the switching region. Therefore, the reliability and repeatability of this process justifies its use to enable large area solution-processed printed circuits at the cost of reduced mobility.

Keywords: TIPS-pentacene; micro-dispensing; Marangoni flow; printed electronics

1. Introduction

A lot of attention has been paid to solution processed 6,13-Bis(triisopropylsilylethynyl)pentacene (TIPS-pentacene) due to the promise that it holds for enabling cost effective printed electronics in application fields such as printed RFID labels [1,2], smart packaging [3], disposable electronic circuit boards [4] *etc.* Although a lot of research has been published on the advances of using printed TIPS-pentacene in which different research groups have built organic field-effect transistors (OFET) with mobility in the saturation regime greater than $1 \text{ cm}^2/\text{Vs}$ [5,6], most organic semiconductor (OSC) circuitry is still based on evaporated pentacene due to the reproducibility and homogeneity of the results. This is due to the inherent problem that plagues TIPS-pentacene and other such small molecule semiconductors that the poor control of the phase distribution and morphology leads to a wider disparity in the device-to-device performance [7].

Ink jetting of OSCs such as TIPS-pentacene and thiophenes by other research groups have shown that the absolute device performance and the grouping of the results are dependent primarily on the surface energy of the substrates, the drying conditions, the choice of solvents and the concentration of the solute in the solvents [8–10]. Lim *et al.*, have furthered the understanding of the relationship between the film morphologies and crystallization due to a two-solvent drying process [11]. Additionally, the research group of Maria Lada *et al.* have also published a method to increase the mobility of TIPS-pentacene via a dual solvent crystallization process [12]. Similarly, Gil Jo Chae *et al.* have also focused on improved performance in TIPS-pentacene using solvent additives such as diphenyl ether (DPE) or chloronaphthalene (CN) [13]. We have further developed and utilized these concepts to enable a reliable and repeatable dispensing system for TIPS-pentacene. The focus of our work is targeted at the optimization procedure that enables the maximum reproducibility rather than searching for the best possible OFET performance parameters. The main focus is to enable a high throughput Roll-to-Roll (R2R) compatible process, where reliability, reproducibility and intra-device variation is of prime importance, rather than absolute mobility values.

In μ -dispensing of OSCs one of the biggest challenges is to overcome the concentric ring-like deposits that are created due to the convective flow during the drying process. This is evident also as thick rings at the edges of the drop, commonly referred to as the “coffee-stain” effect [14,15]. The starting point is the research done by research groups [11–14,16,17] to solve this problem by use of a mixed solvent system. By using a mixed solvent system besides the existence of a convective flow in the drying droplet, there is the creation of a Marangoni flow due to the difference in boiling points and surface tension of the solvents. This Marangoni flow can be chosen by careful selection of the solvent components to either counteract the convective flow process or to enhance it.

As put forth by the research group of Lim *et al.* [11], the choice of major to minor solvent ratio, whereby the Marangoni flow counteracts the convective flow, is defined such that the minor component in the solvent mixture has a higher boiling point and a lower surface tension than the major solvent in the composition. This was the starting point for our research. In this study, we have demonstrated that

the use of *o*-xylene and 1,2-dichlorobenzene (DCB) as major and minor solvents along with the addition of poly(α -methylstyrene) (PAMS) as a binder for TIPS-pentacene [7] leads to a more uniform crystallization in the droplets as compared to other common solvents compatible to a large area Roll-to-Roll (R2R) processing.

2. Two-Solvent Optimization Process and Its Results

2.1. Experimental Part I

Based on the following two criteria that the minor component in the solvent mixture has: (1) a higher boiling point and (2) a lower surface tension than the major solvent in the solvent mixture, along with two additional constraints which were: (1) the solubility of TIPS-pentacene (as shown in Figures 1 and 2a large area processing compatibility in an Roll-to-Roll (R2R) environment, we chose 26 solvent combinations with varying major to minor solvent ratios to initiate characterization of the μ -dispensing process and film morphology. The list of the solvent combinations is shown in Table 1. In this table, all the solvents that are used in the present work, sorted by major and minor solvents, are listed. The basis for the solvent ratios is taken from the research paper of Jung Ah Lim *et al.* [11], where it was inferred that if the boiling point of the two solvents are far apart (temperature difference >20 °C), the minor solvent should have a share in the mixture of 25% or less. On the other hand, if the boiling points are close to one another (temperature difference <20 °C), the minor solvent should have a share between 25% and 50%.

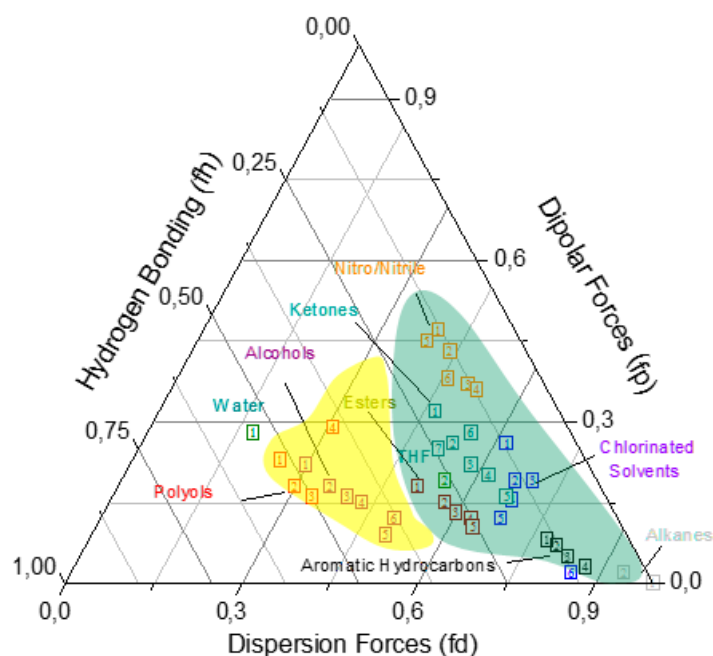


Figure 1. Teas Chart showing the solubility of TIPS-pentacene in common solvent groups.

Using each of these solutions, a 1% (weight) solution of TIPS-pentacene was formulated. Subsequently, the solution was filtered through a $0.45\ \mu\text{m}$ syringe filter and dispensed (volume of $0.3\ \mu\text{L}$) onto a planarized polyethylene naphthalate (PEN) foil substrate. The PEN substrate was mounted onto a carrier wafer to maintain a flat surface. Afterwards, the samples were allowed to dry in the ambient

laboratory air (23 °C and 25% RH) to allow a slow and undisturbed drying process, so that the self-assembly of the small molecules could take place successfully.

After the drops have dried completely, images of the crystallization were taken using a Zeiss Axioplan optical microscope (Carl Zeiss AG, Oberkochen, Germany) in a dark field setting. The dark field setting was preferred as it allows the source light to illuminate the sample and only the scattered light enters the objective and produces the image, whereas the directly transmitted light is omitted. This allowed for a better visualization of the drop crystallization. The results of the complete set are shown in Figure 2.

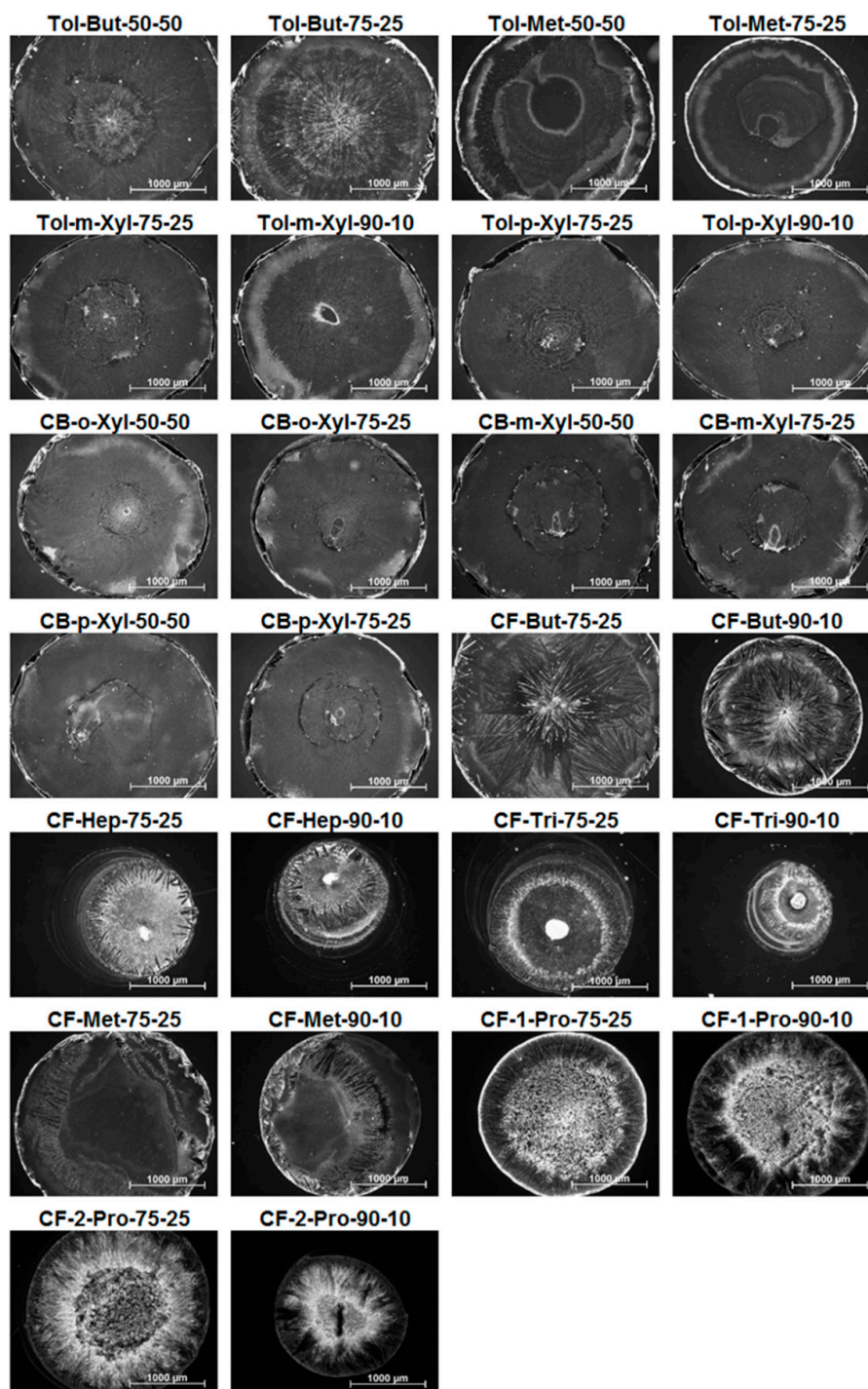


Figure 2. Dark field microscope images of the drop crystallization in each of the 26 solvent mixtures as specified in Table 1.

Table 1. List of the 26 different solvent combinations.

#	Major Solvent	Boiling Point (°C)	Minor Solvent	Boiling Point (°C)	Ratio	Short Name
A1	Toluene	111 °C	<i>n</i> -Butyl acetate	126 °C	50%–50%	Tol-But-50-50
A2	Toluene		<i>n</i> -Butyl acetate		75%–25%	Tol-But-75-25
A3	Toluene		4-Methyl-2-pentanone	117 °C	50%–50%	Tol-Met-50-50
A4	Toluene		4-Methyl-2-pentanone		75%–25%	Tol-Met-75-25
A5	Toluene		<i>m</i> -Xylene	139 °C	75%–25%	Tol- <i>m</i> -Xyl-75-25
A6	Toluene		<i>m</i> -Xylene		90%–10%	Tol- <i>m</i> -Xyl-90-10
A7	Toluene		<i>p</i> -Xylene	138 °C	75%–25%	Tol- <i>p</i> -Xyl-75-25
A8	Toluene		<i>p</i> -Xylene		90%–10%	Tol- <i>p</i> -Xyl-90-10
B1	Chlorobenzene	132 °C	<i>o</i> -Xylene	144 °C	50%–50%	CB- <i>o</i> -Xyl-50-50
B2	Chlorobenzene		<i>o</i> -Xylene		75%–25%	CB- <i>o</i> -Xyl-75-25
B3	Chlorobenzene		<i>m</i> -Xylene	139 °C	50%–50%	CB- <i>m</i> -Xyl-50-50
B4	Chlorobenzene		<i>m</i> -Xylene		75%–25%	CB- <i>m</i> -Xyl-75-25
B5	Chlorobenzene		<i>p</i> -Xylene	138 °C	50%–50%	CB- <i>p</i> -Xyl-50-50
B6	Chlorobenzene		<i>p</i> -Xylene		75%–25%	CB- <i>p</i> -Xyl-75-25
C1	Chloroform	61 °C	<i>n</i> -Butyl acetate	126 °C	75%–25%	CF-But-75-25
C2	Chloroform		<i>n</i> -Butyl acetate		90%–10%	CF-But-90-10
C3	Chloroform		Heptane	98 °C	75%–25%	CF-Hep-75-25
C4	Chloroform		Heptane		90%–10%	CF-Hep-90-10
C5	Chloroform		2,2,4-Trimethylpentane	99 °C	75%–25%	CF-Tri-75-25
C6	Chloroform		2,2,4-Trimethylpentane		90%–10%	CF-Tri-90-10
C7	Chloroform		4-Methyl-2-pentanone	117 °C	75%–25%	CF-Met-75-25
C8	Chloroform		4-Methyl-2-pentanone		90%–10%	CF-Met-90-10
D1	Chloroform	61 °C	1-Propanol	97 °C	75%–25%	CF-1-Pro-75-25
D2	Chloroform		1-Propanol		90%–10%	CF-1-Pro-90-10
D3	Chloroform		2-Propanol	82 °C	75%–25%	CF-2-Pro-75-25
D4	Chloroform		2-Propanol		90%–10%	CF-2-Pro-90-10

An optical evaluation of the crystallization was performed to make a pre-selection of expedient compositions out of the high variety of solvent mixtures. Solvent combinations are referred to as expedients when the drying result exhibit homogeneous and distinct crystal formations. As part of the optical evaluation three compositions meet the requirements: “Tol-But-75-25”, “CB-*o*-Xyl-75-25” and “CF-But-90-10”. The selected solvent mixtures were used for the next experimental step.

2.2. Experimental Part II

In this experimental step, the expedient compositions of experimental step 1 were used and were attempted to be improved. Furthermore, a new solvent pair (*o*-dichlorobenzene with tetralin) was added. Although the temperature difference between toluene and butyl acetate and between chlorobenzene and *o*-xylene is less than 20 °C, the proportion of the minor solvent was further reduced, since the composition of 75% to 25% has shown more promising results for both solutions than the composition of 50% to 50%. The solution of chloroform and butyl acetate (90% to 10%) showed a good semiconductor layer as the drying result and was therefore repeated in this experimental step. Table 2 shows an overview of the combinations and solvent ratios.

The drops were then processed identically to the process mentioned in the experimental part I. After the drops had dried completely, microscope images of the crystallization were taken and is shown in Figure 3, but unlike experimental step I, a bright field setting was chosen as it showed better contrasting

images than the dark field setting for the drop crystallization. The bright field setting here refers to the fact that the samples were illuminated from below, the better contrast in the samples is caused by absorbance as the samples are observed from above.

Table 2. List of the shortlisted solvent combinations for experimental part II.

#	Major Solvent	Boiling Point (°C)	Minor Solvent	Boiling Point (°C)	Ratio	Short Name
A1	Toluene	111 °C	<i>n</i> -Butyl acetate	126 °C	90%–10%	Tol-But-90-10
A2	Toluene		<i>n</i> -Butyl acetate		80%–20%	Tol-But-80-20
B1	Chlorobenzene	132 °C	<i>o</i> -Xylene	144 °C	90%–10%	CB- <i>o</i> -Xyl-90-10
B2	Chlorobenzene		<i>o</i> -Xylene		80%–20%	CB- <i>o</i> -Xyl-80-20
C1	Chloroform	61 °C	<i>n</i> -Butyl acetate	126 °C	90%–10%	CF-But-90-10
D1	<i>o</i> -Dichlorobenzene	180 °C	Tetralin	207 °C	95%–5%	<i>o</i> -DCB-Tet-95-5
D2	<i>o</i> -Dichlorobenzene		Tetralin		90%–10%	<i>o</i> -DCB-Tet-90-10

Analysis of the images of “Tol-But-90-10” and “Tol-But-80-20” show that the crystal growth was directed towards the center. The crystallization is quite closed. A coffee-stain is present. Particularly, in the crystal structure of “Tol-But-80-20”, small gaps were observed along with areas that have no visible deposits, suggesting that there is no semiconductor material.

The semiconductor layer of “CB-*o*-Xyl-90-10” and “CB-*o*-Xyl-80-20” shows a coffee-stain. The coverage crystal growth is not well directed and separated, and curved ring-like areas with crystal deposits can be seen.

The surface layer of “CF-But-90-10” shows strong crystal growth directed from the outside to the inside. They meet and merge in the center of the circle area. However, there are gaps between the crystal structures at the outer edge area.

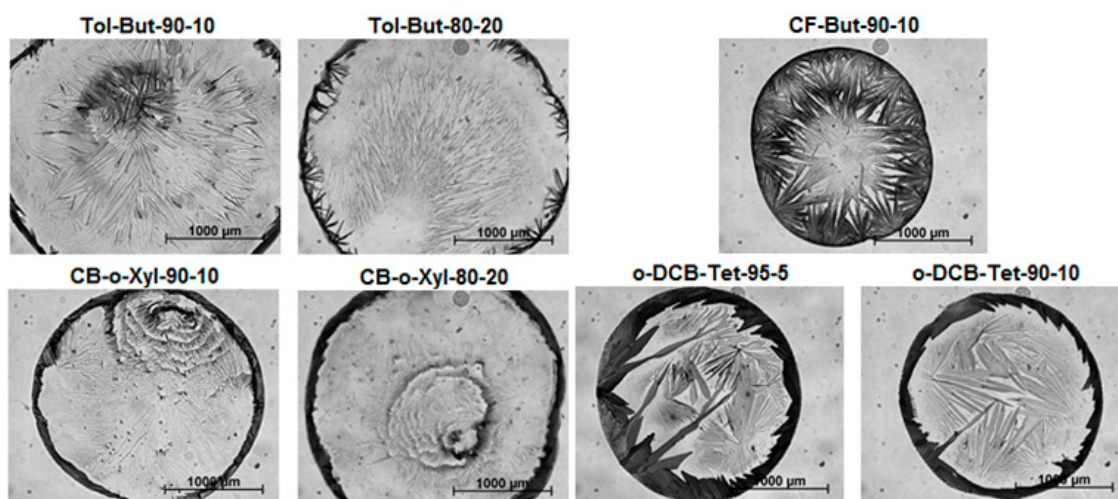


Figure 3. Bright field microscope images of the drop crystallization of the shortlisted solvent mixtures as specified in Table 2.

The drop surfaces of “*o*-DCB-Tet-90-10” shows a thick coffee-stain and distinct crystals directed towards the center, but gaps are visible between the individual crystals. The layer of “*o*-DCB-Tet-95-5”

shows an even thicker coffee-stain from which distinct crystals grow into the circle area. However, in the circle area, there are also many smaller crystallization formation centers that form separate areas.

Figure 4 shows the profilometer $\mu\text{scan}^{\text{®}}$ from NanoFocus AG (NanoFocus AG, Oberhausen, Germany). This non-contact profilometry method enables surface analysis in the micrometer and nanometer ranges [18]. Although some problems did emerge during the measurements due to the PEN substrate properties of transparency and absorbance of part of the light spectrum, it was accurate enough to indicate the discontinuities of the crystal layers. Although only the drop for CF-But-90-10 is shown in Figure 4 to highlight the surface discontinuities, it is to be noted that all the solvent combination except CB-*o*-Xyl suffered from the same problem.

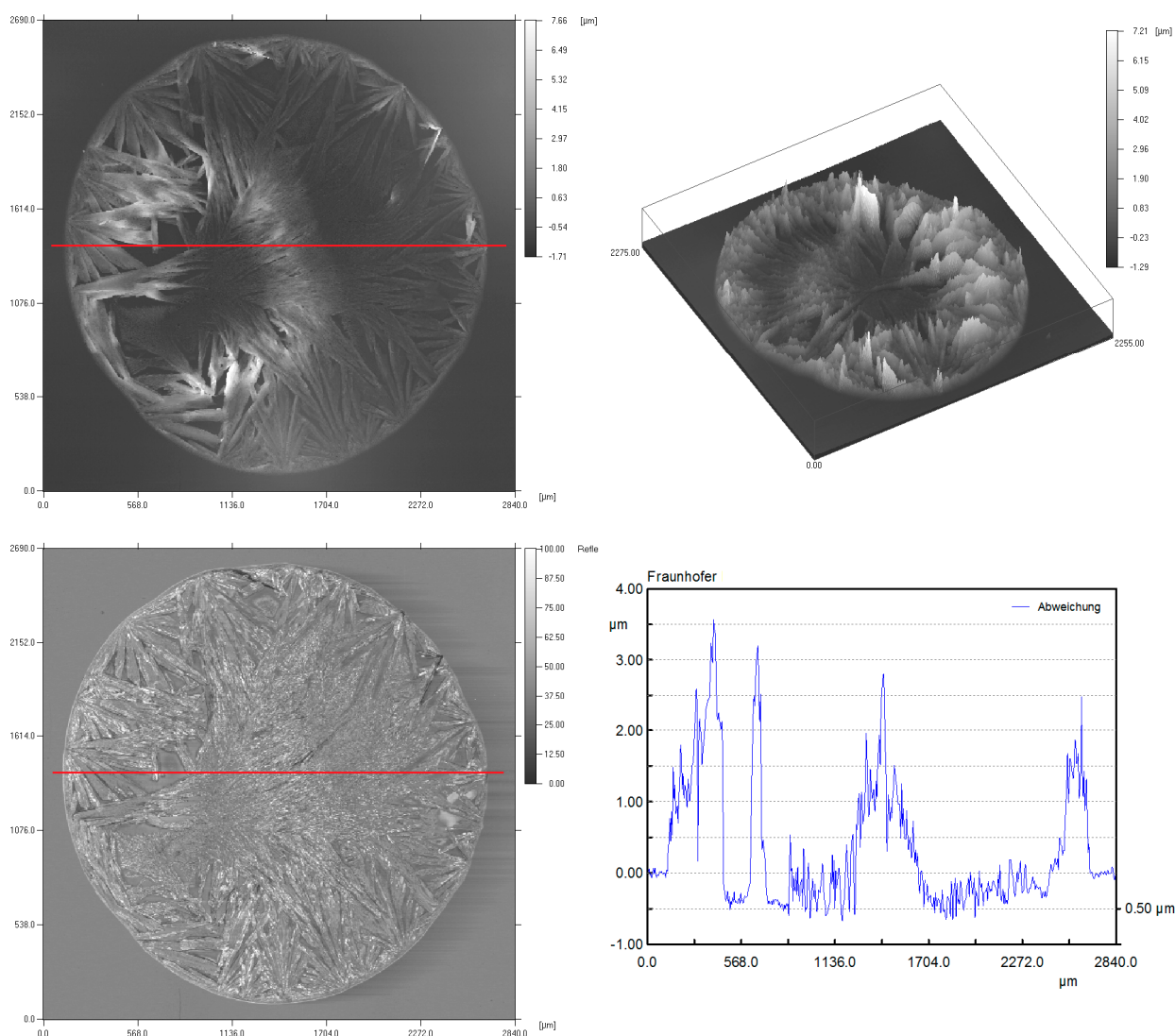


Figure 4. Profilometry results of the CF-But-90-10 drop using a NanoFocus $\mu\text{scan}^{\text{®}}$. It can be seen from the surface profile that the surface is quite rough due to the crystal boundaries and that there are areas where no material is present.

Although the results of Figure 3 show there is a directed growth of the crystal structures, they were far from being either homogenous or reproducible. Additionally, the use of just TIPS-pentacene in the solvent results in discontinuities in the crystal layer, as shown in Figure 4. The profilometry results

further indicate the following: (1) the surface is rather rough *i.e.*, a high degree of variance in the surface morphology due to the crystal structures; (2) the layer is discontinuous *i.e.*, areas are present with no OSC material on the surface; (3) the surface thickness is too high to be viably used in an organic thin film transistor (OTFT) configuration.

2.3. Experimental Part III

To consequently tackle the problem of surface discontinuities, it was decided to use two insulating binders directly in the solvent mixture to improve surface homogeneity. The two chosen binders were: (1) polystyrene (PS) and (2) PAMS. One percent (by weight) of the two binders were added to three of the shortlisted solvent mixtures from experimental part II respectively. The shortlisted solvent mixtures from experimental part II were: (1) Tol-But-90-10, (2) CF-But-90-10 and (3) *o*-DCB-Tet-90-10. The solvent mixtures and binder details are shown in Table 3.

Table 3. List of the three sets of short listed solvent combinations for experimental part III.

#	Major Solvent	Boiling Point (°C)	Minor Solvent	Boiling Point (°C)	Ratio	TIPS-pentacene	Binder
A1	Toluene		<i>n</i> -Butyl acetate		90%–10%	1%	None
A1_PS	Toluene	111 °C	<i>n</i> -Butyl acetate	126 °C	90%–10%	1%	PS (1% wt)
A1_PAMS	Toluene		<i>n</i> -Butyl acetate		90%–10%	1%	PAMS (1% wt)
C1	Chloroform		<i>n</i> -Butyl acetate		90%–10%	1%	None
C1_PS	Chloroform	61 °C	<i>n</i> -Butyl acetate	126 °C	90%–10%	1%	PS (1% wt)
C1_PAMS	Chloroform		<i>n</i> -Butyl acetate		90%–10%	1%	PAMS (1% wt)
D1	<i>o</i> -Dichloro benzene		Tetralin		90%–10%	1%	None
D1_PS	<i>o</i> -Dichloro benzene	180 °C	Tetralin	207 °C	90%–10%	1%	PS (1% wt)
D1_PAMS	<i>o</i> -Dichloro benzene		Tetralin		90%–10%	1%	PAMS (1% wt)

The results of experimental part III, as shown in Figure 5, shows an improvement of the surface continuity for each combination with a binder when compared to one without the use of a binder. In addition, the profilometry results as shown in Figure 6, further validate that the adding of the binder solves the surface discontinuity problem. The drops of A1_PS, C1_PS and D1_PAMS (refer to Table 3) are the ones with the most continuous drop surfaces of the whole set. These results show that the addition of the binder solves one of the problems *i.e.*, the surface discontinuity problem as faced in the experimental part II.

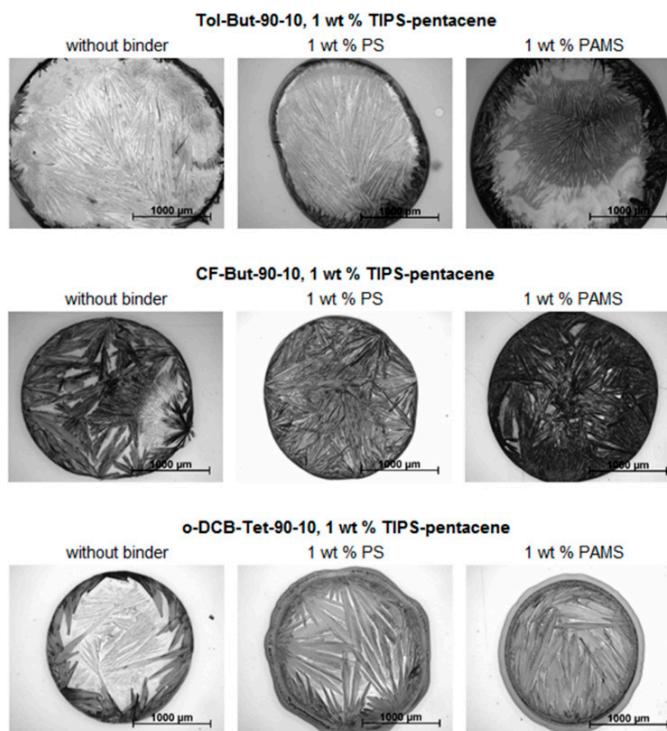


Figure 5. Microscope images of drops of experimental part III with and without binders.

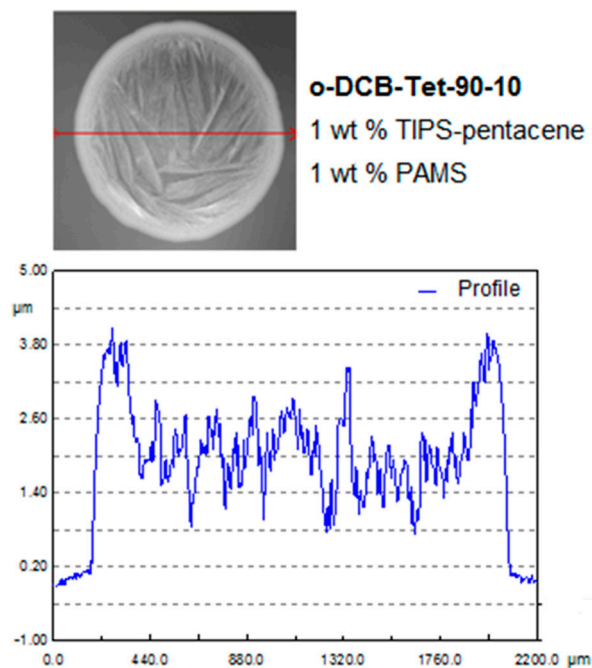


Figure 6. Profilometry results of the D1_PAMS drop. It can be seen that the surface still exhibits discontinuities at the crystal boundaries.

The problem that could not be addressed effectively with these solvent mixtures is the repeatability in the drop crystallization. When a set of these drops was dispensed onto the substrate, the crystallization growth appeared to be different in each dried drop. The crystal growth process was not fully repeatable. This problem is exemplified in Figure 7, where nine drops of the D1_PAMS solution were μ -dispensed onto the PEN substrate. The crystallization albeit improved and better packed in terms of fewer surface

discontinuities suffers from a large inter-drop variation, albeit our best efforts in the variation in crystallization could not be improved.



Figure 7. Microscope images of nine D1_PAMS drops indicating the variance in crystallization repeatability.

2.4. Experimental Part IV

With a view to improve the repeatability of the dispensing process, we made a modification to the solvent pair after evaluation of all of the results of the three experimental parts above. The selection criteria of the major and minor solvent was modified such that the difference between the boiling points of the minor solvents to major components is made as higher. In selecting *o*-Xylene as the major solvent and *o*-Dichlorobenzene as the minor solvent in the solvent mixture, the resulting mixture has the property that the minor component in the solvent mixture has a higher boiling point and a higher surface tension than the major solvent. Table 4 details the solvent mixture. This solution mixture was then optimized by the same process as described in the three experimental parts above and the μ -dispensed drop results are shown in Figure 8. From Figure 8, it is evident that the combination of *o*-Xylene (75% by volume) with *o*-Dichlorobenzene (25% by volume) in which 1.5% (by weight) TIPS-pentacene and 1.5% (by weight) PAMS is dissolved, produces the desired crystallization results. Here, it can be seen that the crystals grow in a homogenous manner from the edge of the drops converging towards the center. The crystals also appear to be tightly packed leaving no discontinuities on the film surface.

Table 4. Selected solvent mixture pair for experimental part IV and their properties.

Type	Name	Boiling Point (°C)	Surface Tension @ 20 °C (dyn/cm)
Major Solvent (75%)	<i>o</i> -Xylene	144.4	30.53
Minor Solvent (25%)	<i>o</i> -Dichlorobenzene	180.5	37

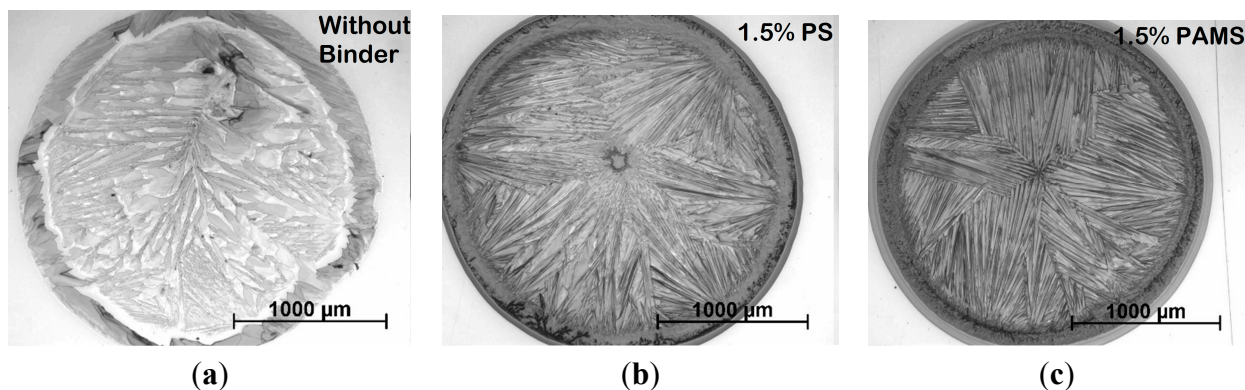


Figure 8. Microscope images of the drops of experimental part IV (a) without binder, (b) with 1.5% (wt) PS and (c) with 1.5% (wt) of PAMS.

Figure 9 shows the reproducibility of the process using this improved solvent mixture. Here, it can be seen that this solvent mixture is superior to all the previous solutions tried out in this paper. It effectively solves the problem of homogenous crystal growth and is reliably reproducible.



Figure 9. Microscope images of the drops from experimental part IV indicating a high degree of reproducibility in the different dispensed drops.

However, for these drops to be viably used in OTFTs, their film thickness needs to be reduced. To enable the reduction in film thickness and to allow for a uniform surface thickness, the concentration of the TIPS-pentacene was reduced in the solution, keeping the other components the same. Figure 10 shows the results of the profilometry results and microscopic images of the drops at concentration levels varying from 1.5% to 0.125% of TIPS-pentacene. Correspondingly, the layer thickness varied from about 2 μm to 300 nm. Using the 0.125% concentration solution, we were able to create ~ 300 nm thick layers without any discontinuities. It is to be noted that one side effect of the reduction in concentration is the increase in diameter of the dispensed drops although the same volume was dispensed of each solution.

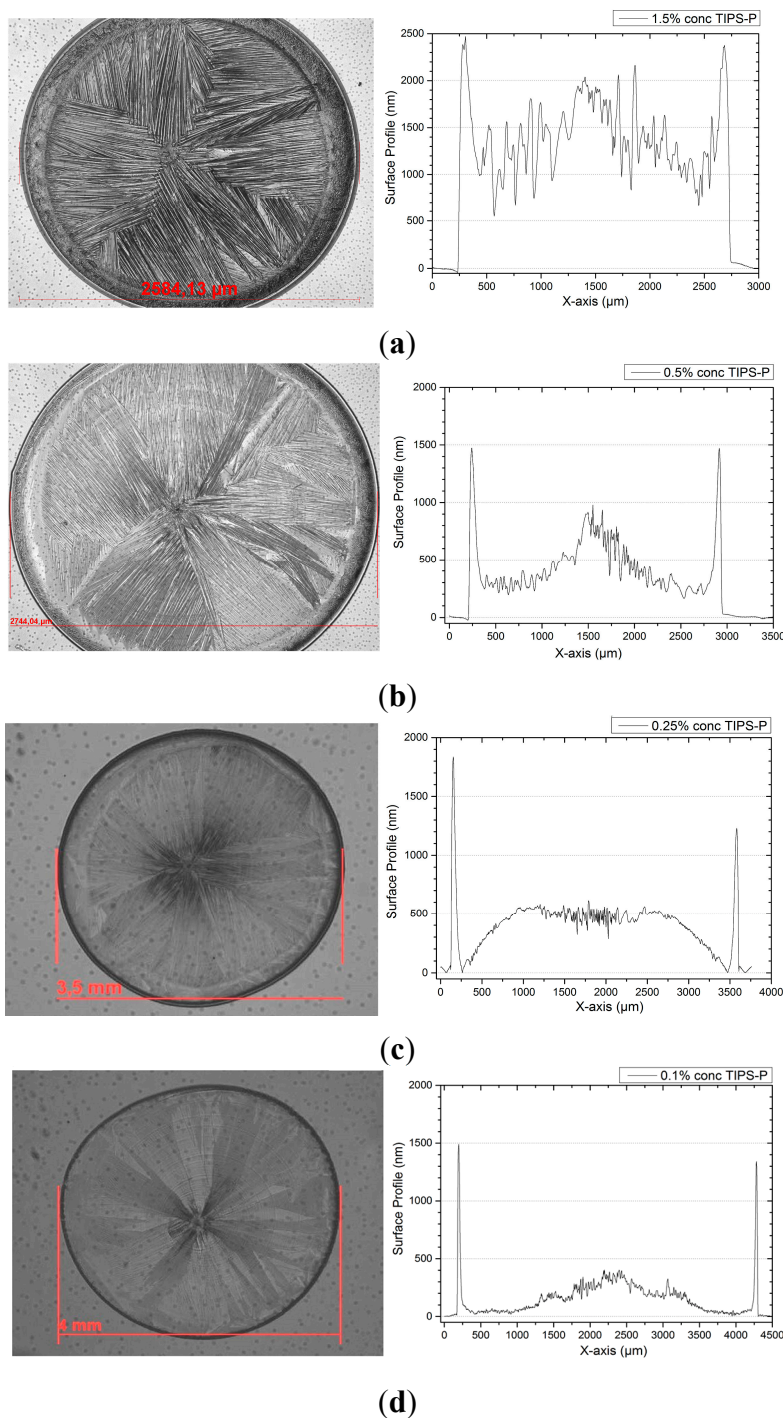


Figure 10. Microscope images of the drops and their corresponding profilometry results with the conc. of TIPS-pentacene varying from (a) 1.5%, (b) 0.5%, (c) 0.25% and (d) 0.125%.

3. Results of the OFETs

OFETs were fabricated using this solvent mixture. The OFET stack is schematically presented in Figure 11. Here, a PEN foil was laminated onto a silicon carrier wafer, following this, a layer of SU-8 (MicroChem, Westborough, MA, USA) is spin coated onto the surface and cured. This acts as a planarization layer of the PEN foil onto which aluminium gate structures were deposited. The aluminium gate was deposited through an electron beam evaporation process through a shadow mask. The dielectric

layer of SU-8 is spin coated onto the surface and has a thickness of 300 nm. The TIPS-pentacene solution is then μ -dispensed onto the surface. The drops were allowed to air dry in the ambient laboratory conditions and after were then tempered at 110 °C for a period of 10 min. Gold acting as the source drain electrodes were deposited via a thermal evaporation process through a shadow mask. The OFET structures were then characterized using a semiconductor parameter analyzer (Keithley 4200, Keithley Instruments, Solon, OH, USA) without any further encapsulation layer.

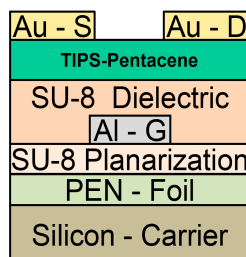


Figure 11. Schematic diagram of the OFET stack used for testing the ideal solvent mixture from experimental part IV for the micro-dispensed TIPS-pentacene based transistors.

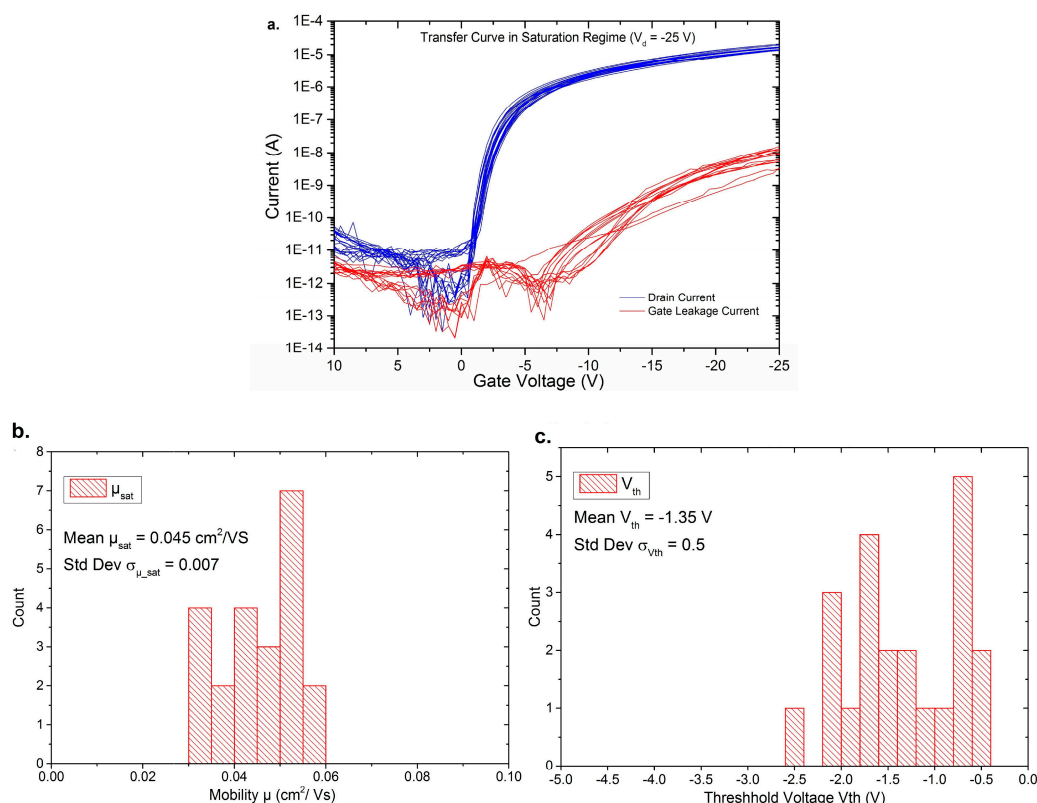


Figure 12. Plot showing the tight grouping of the (a) transfer curves and the histogram results of (b) the mobility in the saturation regime and (c) the threshold voltage.

Figure 12 shows the results of 20 transfer curves from these OFET devices. Here, the drain voltage V_d was maintained at -25 V, whereas the gate voltage V_g was swept from 10 V to -25 V. It can be seen from the tight grouping of these OFET results that the whole process is quite reproducible and repeatable. The mean average saturation mobility for these OFETs was 0.045 cm^2/Vs , whereas the mean average

threshold voltage V_{th} was at -1.35 V. The ratio between the drain current in saturation and the gate leakage current is 10^3 .

Another interesting result that can be observed is that the OFETs display almost no hysteresis in the transfer curves measured in both the saturation and linear regime (Dual Sweep) which is shown in Figure 13.

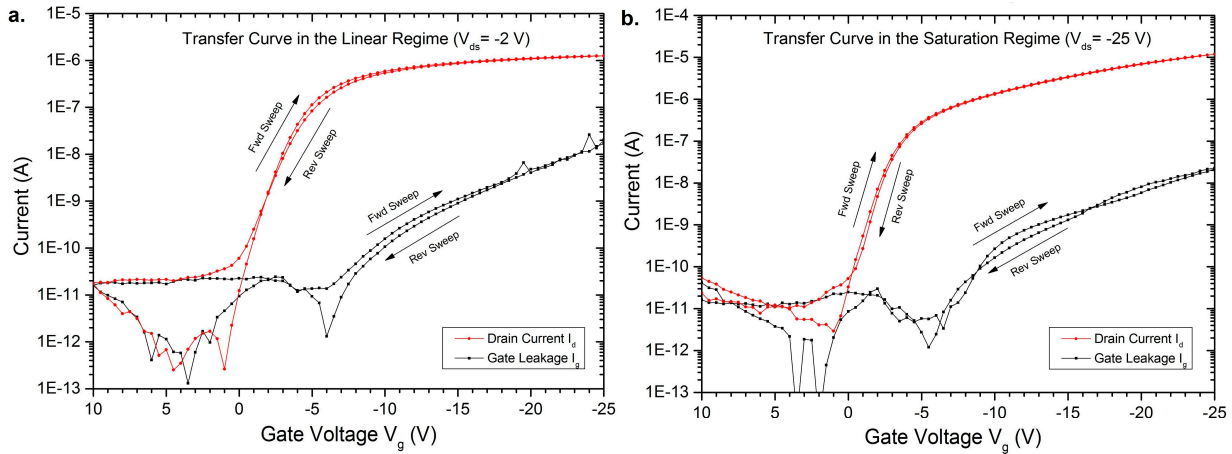


Figure 13. Graph indicating the low hysteresis in the transfer curves in (a) linear regime and in the (b) saturation regime.

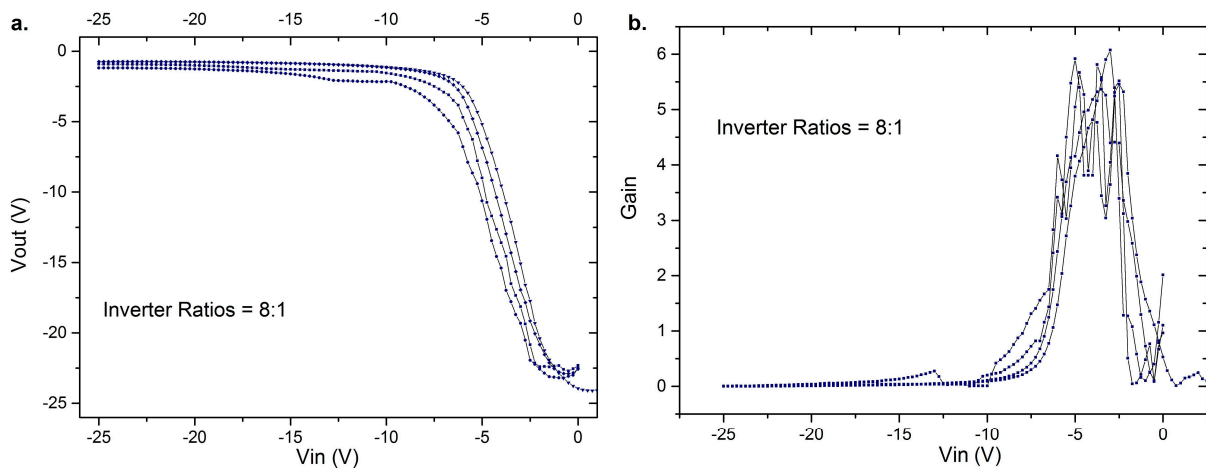


Figure 14. Inverter curve showing the (a) switching characteristics and (b) the gain plot for 4 inverters in the switching region.

Here, it can be observed that the hysteresis is near non-existent in these OFETs. This could be due to a variety of reasons including the choice of the SU-8 dielectric as well as the crystal ordering during the drying process. Increased hysteresis issues have been identified in the transfer curves in prior investigations using a semiconducting polymer due to charge traps at the semiconductor/dielectric interface originated from dielectric surface functionalities, adsorbed small molecules at the interface or structural defects of the semiconductor [19]. The absence of a hysteresis indicates a well-ordered layer of the TIPS-pentacene at the semiconductor/dielectric interface with minor defects and thus low density of charge carrier trapping sites.

P-type inverters were implemented using these OFETs, wherein the driver: load transistor ratio was maintained at 8:1. The inverter curves and the gain plot are shown in Figure 14. In the switching region

between -7 V and -2.5 V, the inverter gain is over 4. This shows that these OFETs are suitable to be used as ring oscillators and flip-flops.

4. Conclusions

In this paper, we have developed a process to show the importance of creating a uniform crystallization in the TIPS-pentacene layer to produce reliable and repeatable OFET performances. The process is a modification of the traditional two solvent drying process using the Marangoni flow to counteract the convective flow in a drying droplet. It was optimized to enable a complete Roll-to-Roll processing of the samples and to create printed inverters.

The goal of this process was to increase the repeatability of the OFET performance as a trade-off to the absolute performance of the individual devices. The mixing of the insulating binder into the solvent mixture goes in the direction of increasing homogeneity of the μ -dispensing results at the cost of reduced mobility. However, for most intended applications, the mobility (in saturation) of 0.045 cm²/Vs is sufficient to enable the use of these transistors in disposable sensors *etc.*, where the performance is not the main criteria but reduction in intra-transistor variance is the main goal.

The results show promise that a large-area solution-processed Roll-to-Roll OFET circuit can be achieved with the use of TIPS-pentacene in a controlled and repeatable μ -dispensed process with relatively large (3–4 mm) active transistor areas reliably. Hence, the reliability and repeatability of this process justifies its use to enable large area solution-processed printed circuits at the cost of reduced mobility.

Acknowledgments

This work was fully supported by the Inno (vation) Flex research program run by the Fraunhofer EMFT in Munich. The authors would like to thank Bill MacDonald and Keith Kilmartin from DuPont Teijin Films for providing the self-adhesive PEN foils.

In addition, the authors would also like to thank Anna Ohlander, Gerhard Klink, Dieter Bollmann and Dieter Hemmetzberger of the Fraunhofer EMFT in Munich for their contributions that enabled this research.

Author Contributions

Indranil Bose was the lead researcher for this paper. He was involved in all aspects of the research for this paper. Kornelius Tetzner was responsible for dielectric and OFET fabrications. He also provided input for the processing of the foil-on-carrier process. Kathrin Borner performed all the chemical formulations and dispensing steps as well the microscope images. This research formed a part of her master thesis at the University of Applied Sciences in Munich. Karlheinz Bock was the research group head, who provided guidelines, specifications and objectives for the work. He also structured and approved the paper, its results and also provided the comparative analysis to the state-of-the-art, thereby making this a focused piece of research.

Conflicts of Interest

The authors declare no conflict of interest.

References

1. Kawase, T.; Moriya, S.; Newsome, C.J.; Shimoda, T. Inkjet printing of polymeric field-effect transistors and its applications. *Jpn. J. Appl. Phys. Part 1* **2005**, *44*, doi:10.1143/JJAP.44.3649.
2. De Gans, B.J.; Duineveld, P.C.; Schubert, U.S. Inkjet printing of polymers: State of the art and future developments. *Adv. Mater.* **2004**, *16*, 203–213.
3. Kippelen, B. Advancing consumer packaging through printable electronics. In Proceedings of the IPST Executive Conference, Atlanta, GA, USA, 9–10 March 2011.
4. Sekitani, T.; Zschieschang, U.; Klauk, H.; Someya, T. Flexible organic transistors and circuits with extreme bending stability. *Nat. Mater.* **2010**, *9*, 1015–1022, doi:10.1038/nmat2896.
5. Park, S.K.; Anthony, J.E.; Jackson, T.N. Solution-processed TIPS-pentacene organic thin-film-transistor circuits. *IEEE Electron Device Lett.* **2007**, *28*, 877–879.
6. Ohe, T.; Kuribayashi, M.; Yasuda, R.; Tsuboi, A.; Nomoto, K.; Satori, K.; Itabashi, M.; Kasahara, J. Solution-processed organic thin-film transistors with vertical nanophase separation. *Appl. Phys. Lett.* **2008**, *93*, doi:10.1063/1.2966350.
7. Hwang, D.K.; Fuentes-Hernandez, C.; Berrigan, J.D.; Fang, Y.; Kim, J.; Potscavage, W.J.; Cheun, H.; Sandhage, K.H.; Kippelen, B. Solvent and polymer matrix effects on TIPS-pentacene/polymer blend organic field-effect transistors. *J. Mater. Chem.* **2012**, *22*, 5531–5537.
8. Plötner, M.; Wegener, T.; Richter, S.; Howitz, S.; Fischer, W.J. Investigation of ink-jet printing of poly-3-octylthiophene for organic field-effect transistors from different solutions. *Synth. Met.* **2004**, *147*, 299–303, doi:10.1016/j.synthmet.2004.05.034.
9. Volkman, S.K.; Molesa, S.; Mattis, B.; Chang, P.C.; Subramanian, V. Inkjetted organic transistors using a novel pentacene precursor. *Mater. Res. Soc. Symp. Proc.* **2003**, *771*, doi:10.1557/PROC-771-L12.7/H11.7.
10. Chang, P.C.; Molesa, S.E.; Murphy, A.R.; Frechet, J.M.J.; Subra manian, V. Inkjetted Crystalline Single-Monolayer Oligothiophene OTFTs. *IEEE Trans. Electron Devices* **2006**, *53*, 594, doi:10.1109/TED.2006.870885
11. Lim, J.A.; Lee, W.H.; Lee, H.S.; Lee, J.H.; Park, Y.D.; Cho, K. Self-organization of ink-jet-printed triisopropylsilylethynyl pentacene via evaporation-induced flows in a drying droplet. *Adv. Funct. Mater.* **2008**, *18*, 229–234; doi:10.1002/adfm.200700859.
12. Lada, M.; Starink, M.J.; Carrasco, M.; Chen, L.; Miskiewicz, P.; Brookes, P.; Obarowska, M.; Smith, D.C. Morphology control via dual solvent crystallization for high-mobility functionalized pentacene-blend thin film transistors. *J. Mater. Chem.* **2011**, *21*, 11232–11238, doi:10.1039/c1jm11119a.
13. Chae, G.J.; Jeong, S.H.; Baek, J.H.; Walker, B.; Song, C.K.; Seo, J.H. Improved performance in TIPS-pentacene field effect transistors using solvent additives. *J. Mater. Chem. C* **2013**, *1*, 4216–4221, doi:10.1039/c3tc30506f.

14. Deegan, R.D. Pattern formation in drying drops. *Phys. Rev. E* **2000**, *61*, doi: 10.1103/PhysRevE.61.475
15. Deegan, R.D.; Bakajin, O.; Dupont, T.F.; Huber, G.; Nagel, S.R.; Witten, T.A. Capillary flow as the cause of ring stains from dried liquid drops. *Nature* **1997**, *389*, 827–829, doi:10.1038/39827.
16. Tekin, E.; Smith, P.J.; Hoepfner, S.; van den Berg, A.M.J.; Susha, A.S.; Rogach, A.L.; Feldmann, J.; Schubert, U.S. Inkjet Printing of Luminescent CdTe Nanocrystal–Polymer Composites. *Adv. Funct. Mater.* **2007**, *17*, 23–28, doi:10.1002/adfm.200600587.
17. Arias, A.C.; Daniel, J.; Krusor, B.; Ready, S.; Sholin, V.; Street, R. All-additive ink-jet-printed display backplanes: Materials development and integration. *J. Soc. Inform. Display* **2007**, *15*, 485–490; doi:10.1889/1.2759554.
18. NanoFokus. Available online: <https://www.nanofokus.de/produkte/uscan/mscan-custom/> (accessed on 13 August 2015).
19. Tetzner, K.; Bose, I.; Bock, K. Organic field-effect transistors based on a liquid-crystalline polymeric semi-conductor using SU-8 gate dielectrics on flexible substrates. *Mater.* **2014**, *7*, 7226–7242, doi:10.3390/ma7117226.

© 2015 by the authors; licensee MDPI, Basel, Switzerland. This article is an open access article distributed under the terms and conditions of the Creative Commons Attribution license (<http://creativecommons.org/licenses/by/4.0/>).